Herschel celestial calibration sources

Four large main-belt asteroids as prime flux calibrators for the far-IR/submm range

T. G. Müller (MPE Garching) &

Z. Balog (MPIA), M. Nielbock (MPIA), T. Lim (RAL), D. Teyssier (HSC), M. Olberg (Onsala), U. Klaas (MPIA), H. Linz (MPIA), B. Altieri (HSC), C. Pearson (RAL), G. Bendo (Manchester), E. Vilenius (MPE)

New thermophysical model solutions for (1) Ceres, (2) Pallas, (4) Vesta, and (21) Lutetia allow to predict highly accurate (<5%) far-IR/submm fluxes (out to about 700 µm). The four objects connect and bridge nicely the absolute stellar reference system in the mid-IR with the planet-based calibration at sub-mm/mm wavelengths.

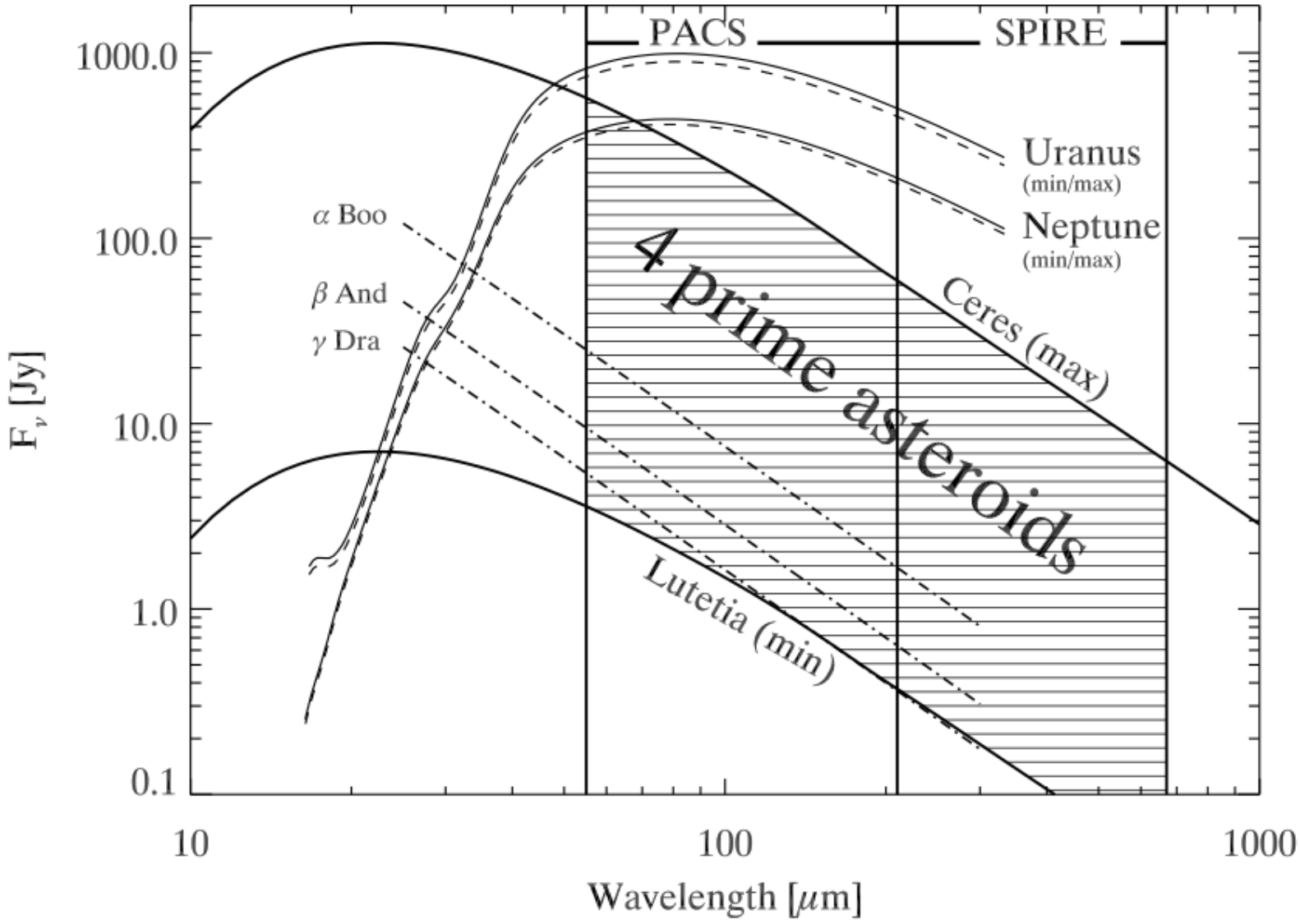

Fig. 1 Overview with the flux densities of the different far-IR/sub-mm/mm calibrators. The Uranus and Neptune SEDs represent the minimum and maximum fluxes during Herschel visibility phases. Three fiducial stars are also shown, their flux coverage is representative for the brightest stellar calibrators. For Ceres and Lutetia we show the minimum and maximum fluxes during Herschel observations.

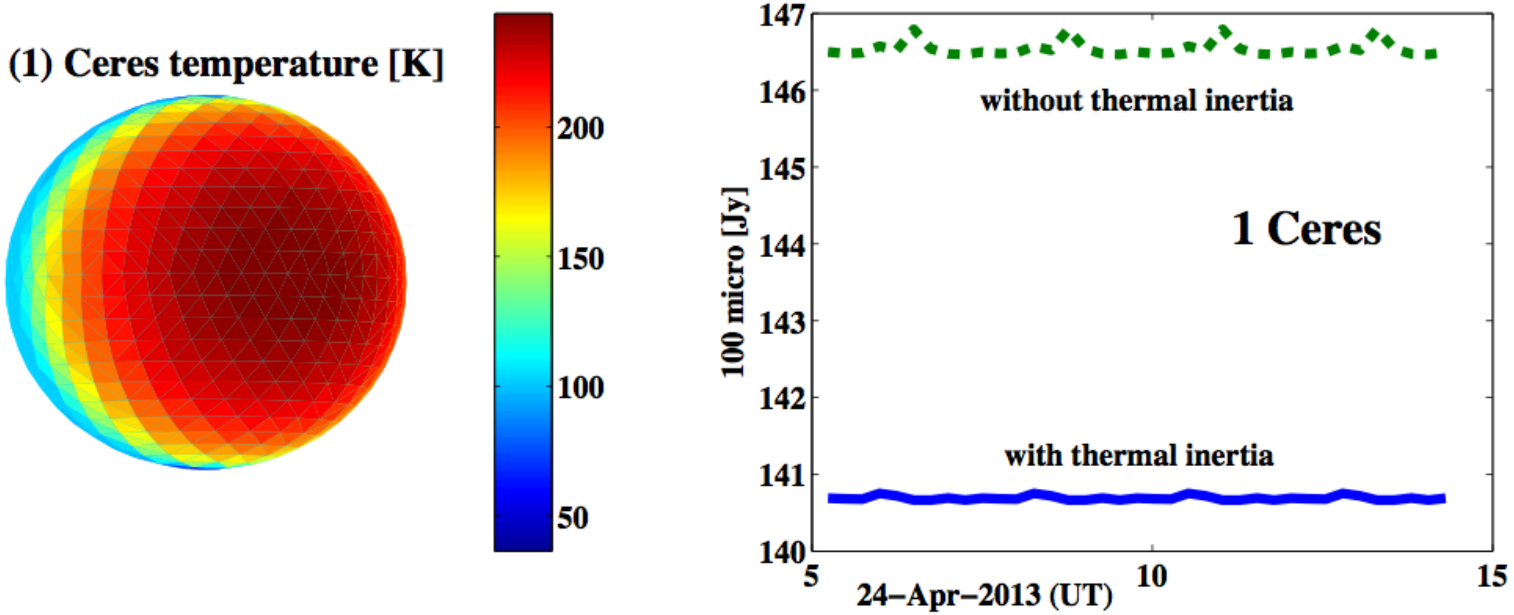

Fig. 2 Left: Shape model of Ceres with the TPM temperature coding on the surface, calculated for the Herschel point-of-view on OD 1441, OBSID 1342270856, rotation axis is along the vertical direction. Right: the corresponding thermal light-curve at 100 μm with and without thermal effects included.

Table 1 Overview (1) Ceres.

effective diameter	D_{eff}	952.4 ± 3.4 km	[78]
shape model	oblate spheroid	a/b=1.0; b/c=1.072	[42,78,7,17]
shape model origin	HST, occultation, AO measurements, lightcurves, ...		
max. lightcurve amplitude	Δ_{mag}	≤0.04	[46]
geometric albedo	p_V	0.090 ± 0.0055	[37,17]
spin axis	$(\lambda_{ecl}, \beta_{ecl})$	(346°, +82°)	[17]
rotation period	P_{sid}	9.074170 ± 0.000001 h	[10]
absolute magnitude	H_V	3.28 mag	[30,46]
slope parameter	G	0.05	[30,46]

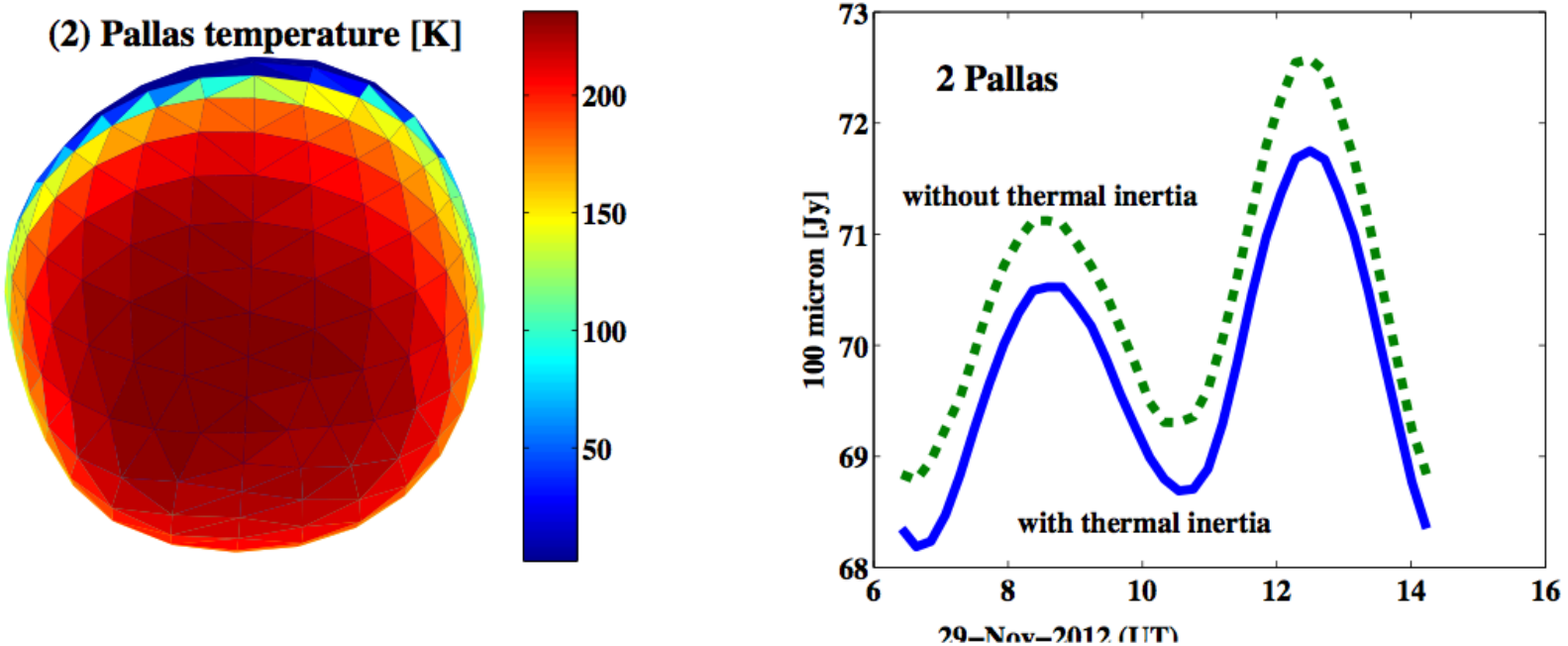

Fig. 3 Left: Shape model of Pallas with the TPM temperature coding on the surface, calculated for the Herschel point-of-view on OD 1295, OBSID 1342256236, rotation axis is along the vertical direction. Right: the corresponding thermal light-curve at 100 μm with and without thermal effects included.

Table 2 Overview (2) Pallas.

effective diameter	D_{eff}	533 $\pm$ 6 km	[18]
shape model	nonconvex shape	a/b=1.06; b/c=1.09	[DAMIT]
shape model origin	HST, occultation, AO measurements, lightcurves, ...		
max. lightcurve amplitude	Δ_{mag}	$\leq$0.16	[31]
geometric albedo	p_V	0.139	[here]
spin axis	$(\lambda_{ecl}, \beta_{ecl})$	(31°, -16°)	[DAMIT]
rotation period	P_{sid}	7.81322 h	[DAMIT]
absolute magnitude	H_V	4.13 mag	[30,46,31]
slope parameter	G	0.16	[30,46,31]

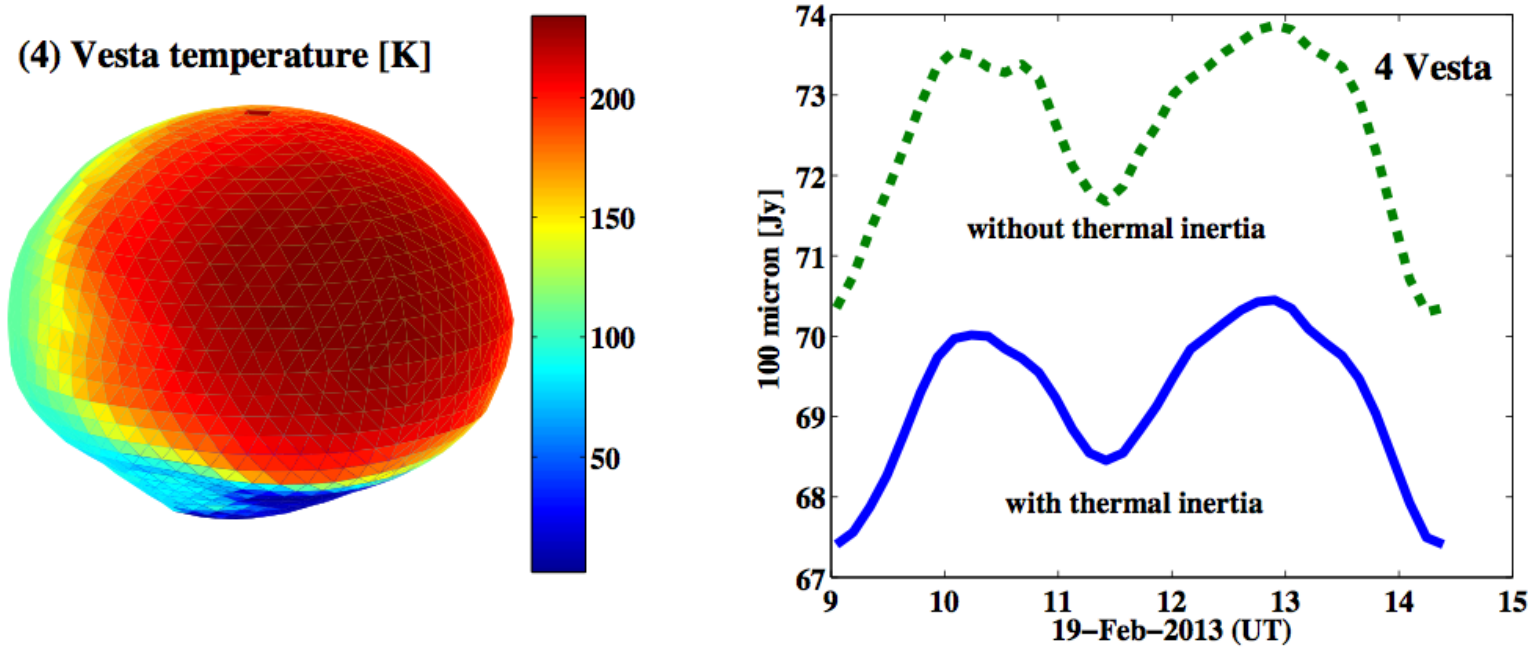

Fig. 4 Left: Shape model of Vesta with the TPM temperature coding on the surface, calculated for the Herschel point-of-view on OD 1377, OBSID 1342263924, rotation axis is along the vertical direction. Right: the corresponding thermal light-curve at 100 μm with and without thermal effects included.

Table 3 Overview (4) Vesta.

effective diameter	D_{eff}	525.4 ± 0.2 km	[70]
shape model	nonconvex shape	a/b=1.03, b/c=1.25	
shape model origin	HST, lightcurves, (DAWN model not yet available)		
max. lightcurve amplitude	Δ_{mag}	$\leq$0.18	[31]
geometric albedo	p_V	0.336	[here]
spin axis	$(\lambda_{ecl}, \beta_{ecl})$	(319°, +59°)	[77]
rotation period	P_{sid}	5.3421289 h	[77,15]
absolute magnitude	H_V	3.20 mag	[46]
slope parameter	G	0.34	[46]

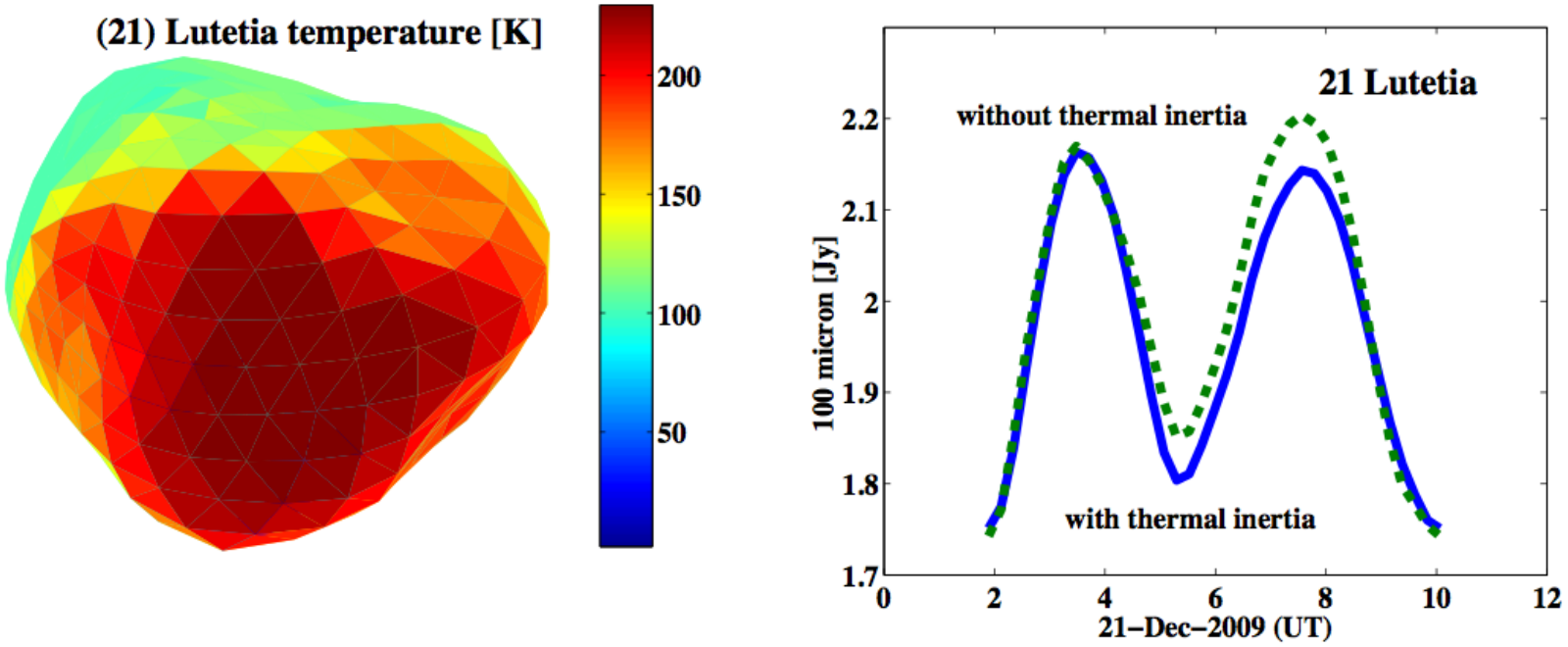

Fig. 5 Left: Shape model of Lutetia with the TPM temperature coding on the surface, calculated for the Herschel point-of-view on OD 221, OBSID 1342188334, rotation axis is along the vertical direction. Right: the corresponding thermal light-curve at 100 μm with and without thermal effects included.

Table 4 Overview (21) Lutetia.

effective diameter	D_{eff}	99.3 km	[9]
shape model	nonconvex shape		[DAMIT]
shape model origin	ROSETTA flyby, occultations, radiometry, lightcurves, ...		
max. lightcurve amplitude	Δ_{mag}	$\leq$0.25	[31]
geometric albedo	p_V	0.19 ± 0.01	[9]
spin axis	$(\lambda_{ecl}, \beta_{ecl})$	(52°, -6°)	[35,9]
rotation period	P_{sid}	8.168271 h	[35,9]
absolute magnitude	H_V	7.25 mag	[4]
slope parameter	G	0.12	[4]

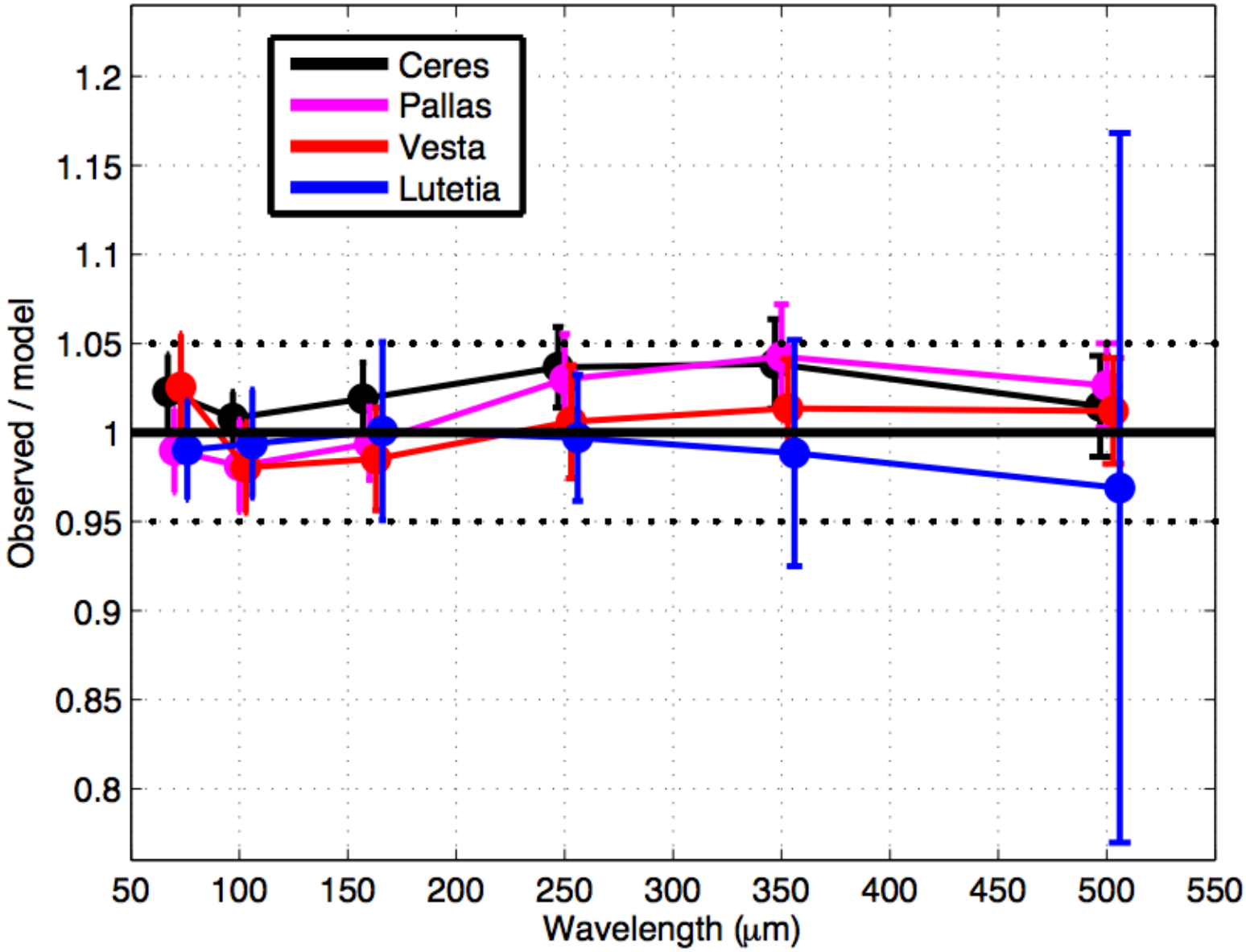

Fig. 10 Dispersion in the ratios of measured-to-model fluxes for the four asteroids as a function of wavelength. The weighted mean ratios are shown with errorbars reflecting the absolute flux calibration of individual measurements as well as the variance of the sample.

For More Information:

Dr. Thomas Müller

Max-Planck-Institut für Extraterrestrische Physik

Giessenbachstrasse

85748 Garching, Germany

http://www.mpe.mpg.de/~tmueller/

tmueller@mpe.mpg.de

Müller, Balog, Nielbock, Lim, Teyssier et al.,
Herschel celestial calibration sources: Four large main-belt asteroids as prime flux calibrators for the far-IR/sub-mm range,
Exp. Astron. (2013), in press